Giant magnetoresistive behavior near the metamagnetic transition in $Ce(Fe_{0.93}Ru_{0.07})_2$

H. P. Kunkel, X. Z. Zhou, and P. A. Stampe
Department of Physics, University of Manitoba, Winnipeg, Canada R3T 2N2

J. A. Cowen and Gwyn Williams
Department of Physics and Astronomy, Michigan State University, East Lansing, Michigan 48824-1116
(Received 20 November 1995; revised manuscript received 4 March 1996)

We present detailed measurements of the field and temperature dependence of the resistivity and magnetization of $Ce(Fe_{0.93}Ru_{0.07})_2$. This system undergoes a ferromagnetic to antiferromagnetic transition near 115 K in zero field; applied fields suppress the temperature at which this transition occurs and a nonconventional giant magnetoresistance results associated with this field-induced suppression. The detailed features in this magnetoresistance are correlated with the corresponding change in the field- and temperature-dependent magnetization, and model calculations attempting to relate these two properties are presented. [S0163-1829(96)05222-8]

I. INTRODUCTION

Stoichiometric $CeFe_2$ appears to be close to an incipient magnetic instability, a proximity inferred not only from the relatively low ferromagnetic ordering temperature ($T_c \sim 230$–240 K) and moment per formula unit ($\mu_{FU} \simeq 2.4\mu_B$) of the parent compound, but also from the ferromagnetic to antiferromagnetic phase transition induced at lower temperature by the substitution of a variety of other (metallic) elements in place of Fe. While the behavior of the parent compound and its associated pseudobinaries have been investigated extensively using a wide range of magnetic, thermal, and transport measurements, the most conclusive evidence supporting the presence of a ferromagnetic-antiferromagnetic transition has been provided by high-resolution neutron diffraction data.[1] Additionally, the latter indicate that the moment rearrangement associated with this transition is accompanied by a structural distortion, both of which appear magnetically driven as ferromagnetic order can be reestablished by the application of a sufficiently large external field.[1]

While the pseudobinaries $Ce(Fe_{1-x}M_x)_2$ (M=Co, Al, Ru, Pd, Rh, etc.) display considerable similarity in aspects of their magnetic/transport behavior, neutron scattering measurements reveal subtle differences, of which the appearance of a Ce moment in the ferromagnetic, but *not* the antiferromagnetic, phase of some (M=Ru) but not all (M=Al,Co) pseudobinaries, and the sharpness of the ferromagnetic to antiferromagnetic transition in systems with M=Ru,Co but with some ''overlap'' in the Al-substituted systems, seem most striking.

Recently, measurements of the magnetoresistance $\rho(H,T)$ and magnetization $M(H,T)$ of the $Ce(Fe_{0.92}Al_{0.08})_2$ and $Ce(Fe_{0.96}Al_{0.04})_2$ systems were reported,[2,3] and these were compared with earlier studies of the zero-field ac susceptibility $\chi_{ac}(0,T)$ of the first sample[4] and the nonlinear magnetic response[5] of the latter sample. From such comparisons it was concluded that amongst macroscopic probes, magnetoresistance measurements appear to provide the clearest indications of the sequential phase transitions displayed by this system. Here we report the results of a similar study, although somewhat more detailed, of $\rho(H,T)$ and $M(H,T)$ in the $Ce(Fe_{0.93}Ru_{0.07})_2$ system, a system in which—according to neutron scattering evidence—the transition to antiferromagnetism is very sharp (in contrast with the Al-substituted pseudobinaries); the present results are also compared with previous, detailed field- and temperature-dependent ac susceptibility measurements on sections of the same sample.[6] The magnetoresistance data again provide a very clear picture of the ferromagnetic to antiferromagnetic transition, with applied fields restoring the ferromagnetic phase—a result most clearly indicated by measurements of the temperature-dependent resistivity in various *fixed* external fields. Magnetoresistance data also show the existence of a giant anomaly (GMR) associated with the field-induced realignment process, and the temperature dependence of the field $H_m(T)$ necessary to induce this metamagnetic transition is estimated in a number of ways and compared with corresponding estimates deduced from magnetization data. These results are discussed below.

II. EXPERIMENTAL DETAILS

The sample used in the present study was taken from a section of the specimen used in a previous ac susceptibility investigation;[6] it had been cut from a larger sample prepared originally by Roy and Coles[7] and used by them for measurements of the zero-field resistivity of various pseudobinaries. Details of the preparation techniques and materials used,[7] along with the annealing procedures,[6] have been discussed previously. The present specimen was in the form of a rectangular bar of approximate dimensions $3.6\times1.5\times1.5$ mm^3 weighing 70.3 mg.

The sample resistance was measured, as a function of applied field (up to 8.5 T) and temperature (1.5 to 125 K), using a high-precision, low-frequency (37 Hz) differential four-probe technique;[8] these measurements were carried out in the longitudinal mode with both the measuring current ($\sim$50 mA) and the field being applied along the largest sample dimension. While this ac technique allows relative resistivity values in the present experiment to be determined with a precision approaching a few parts in 10^5, absolute

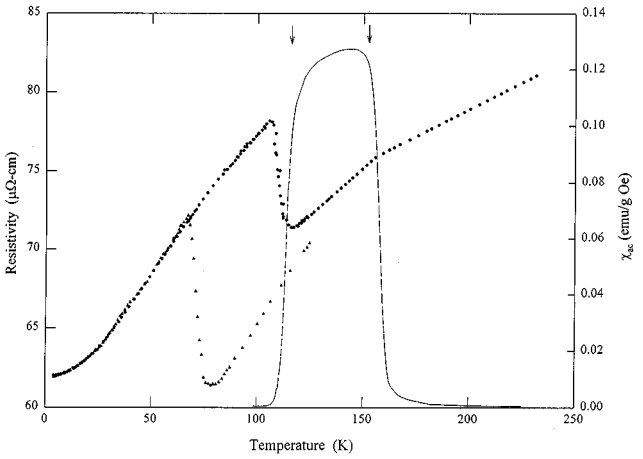

FIG. 1. The resistivity $\rho(H,T)$ (in $\mu\Omega$ cm) plotted against temperature (in K) for fixed applied fields of zero (●) and 7.2 T (▲); the broken line represents the zero-field ac susceptibility (Ref. 6) with the vertical arrows indicating T_c and T_N estimated from these latter data.

resistivities have an estimated uncertainty approaching typically 5–10 %, arising principally from a combination of shape factor and absolute ac voltage errors (this point is discussed in more detail below).

Field- and temperature-dependent magnetization data were acquired using a commercial superconducting quantum interference device (SQUID) magnetometer (a Quantum Design MPMS5 system) with the field applied in the same orientation as for the magnetoresistance studies. A 64-step, 4 cm scan was adopted, and two-scan averaging was implemented. Between each field sweep the sample was warmed above its ferromagnetic ordering temperature, and the magnet reset before cooling in zero field to the next measuring temperature.

III. RESULTS AND DISCUSSION

A. Resistivities in fixed fields

Figure 1 shows the resistivities $\rho(H,T)$ as a function of temperature measured in *fixed* applied fields of $H=0$ and 7.2 T. The dashed curve included in this figure reproduces the previously measured[6] zero-field ac susceptibility while the arrows correspond to the characteristic temperature deduced from the analysis of the detailed field-dependent measurements of the same study. Specifically, the higher-temperature arrow indicates the ferromagnetic ordering temperature T_c ($\simeq 152\pm 1.5$ K) estimated from these magnetic data and the lower arrow designates the temperature of the maximum ($\simeq 112$–117 K) in the coefficient $a_2(T)$ of the leading H^2 term in the field-dependent magnetic response. The former is in good agreement with the temperature (~ 155 K) at which $d\rho/dT$ changes rapidly while the latter is very close to the onset temperature ($\simeq 116$ K) below which an abrupt increase in $\rho(T)$ is evident; this increase is reminiscent of superzone boundary effects, and here the width of the anomaly (i.e., the separation in temperature between maximum and minimum) is approximately 10 K. The correspondence between various features in the transport and magnetic response is particularly reassuring since they were not only derived from different properties but also measured in separate experiments incorporating differing thermometry.

Before discussing the influence of superimposed fields it is appropriate to compare briefly the characteristics of the zero-field resistivity reproduced in Fig. 1 with those reported previously,[7] especially as they involve sections taken from the same sample. While the overall features of these two sets of data are similar, the magnitudes reproduced in Fig. 1 are considerably lower than those estimated previously.[7] However, it appears likely that these differences can be attributed to geometrical/shape factor uncertainties resulting from the presence of microcracks in these rather brittle materials.[7]

That the ferromagnetism to antiferromagnetism transition—and its associated structural distortion—are magnetically driven is confirmed by data acquired in a fixed field of 7.2 T. This field can be seen to depress substantially the onset temperature of the second transition by some 38 K, although the transition width is not affected, the local maximum now appearing near 68 K. The height of the anomaly is, however, enhanced to some 11 $\mu\Omega$ cm compared with a zero-field value of some 7 $\mu\Omega$ cm (this contrasts with the behavior reported for systems like[9] FeRh, in which the magnetoresistance is also associated with a metamagnetic transition, but where there is no such field-induced enhancement), this enhancement resulting from a field-induced suppression of the resistivity associated with the *ferromagnetic* phase as the resistivity of the antiferromagnetic structure, once established, exhibits a weak field dependence. The latter amounts to a small, positive magnetoresistance, not particularly clear in Fig. 1 but amounting to some 3% near 10 K in full field. This behavior is consistent with cyclotron curvature effects as the magnitude of the field-induced increase is roughly comparable with the Kohler-like component observed in Fe-based alloys,[10] scaled for the differences in $\rho(0,T)$. The reduction in the resistivity of the ferromagnetic phase is consistent with a suppression of thermally generated disorder by an applied field below T_c, with the fractional magnetoresistance in a field of 7.2 T, $\Delta\rho(H,T)/\rho(H,T)$ $(=[\rho(0,T)-\rho(H,T)]/\rho(H,T))$, increasing from just over 2% near $T=125$ K to ''giant'' values of around 22% at $T\simeq 80$ K. The variation with temperature of the magnetoresistance is considered in more detail in the following section.

B. Magnetoresistance $\rho(H,T)$

The magnetoresistance data discussed in this section were all acquired in increasing field; the magnetoresistance does display hysteresis, but this is discussed in a later section.

Figure 2 contains the principal results of this section, showing the fractional magnetoresistance $\Delta\rho(H,T)/\rho(0,T)$ at nine different temperatures through the region of the field-induced metamagnetic transition. At temperatures above that for the onset of the transition in zero field (~ 116 K) the magnetoresistance is small and negative ($\Delta\rho/\rho(0,T)\sim -2\%$), in qualitative agreement with the expected field-initiated reduction in the thermally generated orientation disorder in this ferromagnetic regime ($T/T_c\sim 0.8$). On lowering the temperature towards the zero-field onset temperature, this negative component increases slightly, while at and below the onset temperature it increases dramatically. At 114 K, for

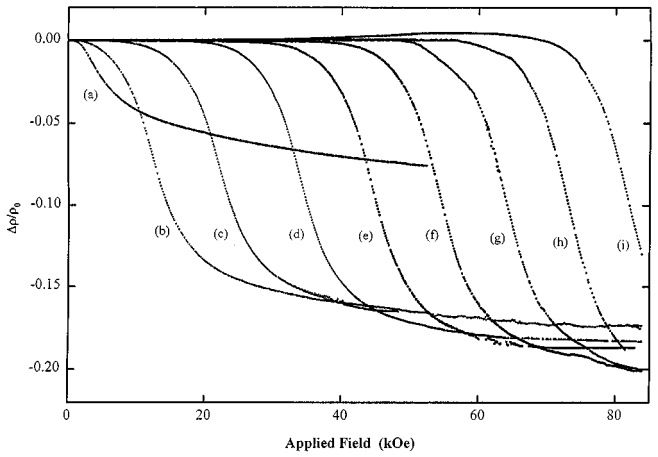

FIG. 2. The magnetoresistance ratio $\Delta\rho/\rho_0$ $[=(\rho(H,T)-\rho(0,T))/\rho(0,T)]$ plotted against applied field (in kOe) at fixed temperatures of (a) 114.1 K, (b) 107.5 K, (c) 101.7 K, (d) 95.3 K, (e) 90.6 K, (f) 84.0 K, (g) 78.2 K, (h) 72.6 K, and (i) 67.0 K.

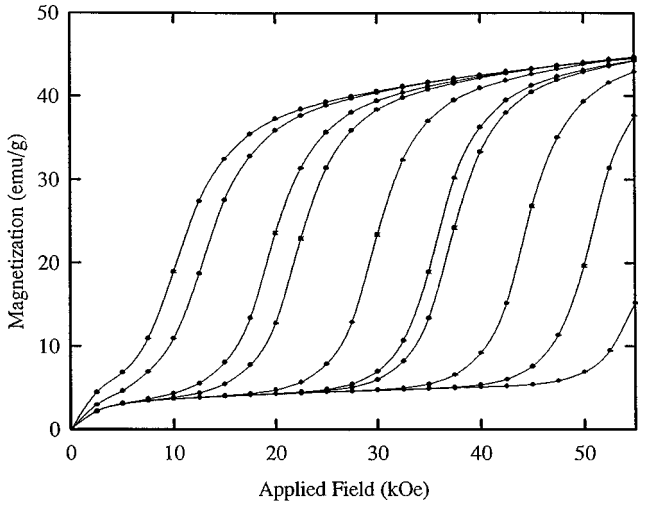

FIG. 3. The magnetization (in emu/g) plotted against applied field (in kOe) at fixed temperatures of (from left to right) 103.8, 101.7, 97.2, 95.3, 89.7, 85.2, 83.9, 78.2, 72.6, and 67.0 K.

example,—curve (a) in Fig. 2—$\rho(0,T)$ has started to climb whereas the resistivity of the field-restored ferromagnetic structure continues to fall, so that the fractional magnetoresistance rises to around -7%. With further reduction in temperature $\rho(0,T)$ and $\rho(H,T)$ continue to diverge—one is essentially moving between the two branches of the resistivity curve shown in Fig. 1—with attendant increases in the magnetoresistance as $\Delta\rho/\rho(0,T)$ climbs to values of around -20% at temperatures below about 105 K. In available fields this behavior persists down to temperatures approaching 78 K [near the minimum in the $\rho(B=7.2\ \mathrm{T})$ vs T curve], below which the full metamagnetic transition cannot be driven by the maximum (8.5 T) field generated by the present magnet; the high-field magnetoresistance then fails to reach saturation—curves (h) and (i) in Fig. 2. Values for the fractional magnetoresistance of -20% or larger are colloquially referred to as ''giant magnetoresistance'' (GMR); here the mechanism for this effect is clear—it is the result of a marked decrease in the resistivity between the antiferromagnetic and the ferromagnetic structures, effected by the application of sufficient large external fields. Further, as the temperature falls throughout the region considered above it is also clear from Fig. 2 that the applied field $H_m(T)$ necessary to initiate the metamagnetic transition increases, exceeding the maximum field available below about 60 K. Before discussing methods for estimating $H_m(T)$ and the growth of this field with decreasing temperature, it is appropriate to discuss features in the magnetization data which are complementary to those outlined above.

C. Magnetization $M(H,T)$

Figure 3 displays the magnetization data acquired on the same sample (with the same orientation) at a number of fixed temperatures, the latter being chosen to match those at which magnetoresistance measurements were taken. These $M(H,T)$ data were all measured in increasing field following zero-field cooling.

At 120 K and above, the *general* features of the M vs H plots resemble those shown in Fig. 3 (the 103.8 K data) (the *detailed* features in the low-field region are however *different*, as discussed later in this section); here the magnetization initially increases rapidly with increasing field, but with a slope (dM/dH) which decreases essentially monotonically. This behavior is similar to that reported[2] for $Ce(Fe_{0.92}Al_{0.08})_2$ at comparable temperatures and is reminiscent of that displayed by canonical inhomogeneous ferromagnets such as AuFe near the percolation threshold.[11] Figure 3 indicates that the magnetization is not saturated at 5.5 T in this temperature range (it approaches a value of 45 emu/g), but a plot of M vs H^{-1} allows an extrapolated estimate for this saturation magnetization to be made ($\sim$49 emu/g), from which a saturated moment of about $2.25\mu_B$ per formula unit is obtained. The latter is close to, but slightly smaller than, the value of $\sim 2.4\mu_B$ per formula unit reported for the parent compound.[12] As the temperature is lowered the initial slope of the magnetization curve falls progressively, so that at 67 K the initial slope [the ratio of M/H in the smallest field (0.25 T) applied in this region] has fallen to around 10^{-3} emu/g Oe. Above this low-field region the magnetization curve flattens, forming a nearly field-independent plateau; the width (in field) of this plateau region is temperature dependent as it terminates with an abrupt increase in the magnetization, signaling the onset of the metamagnetic transition. The field $H_m(T)$ necessary to initiate this antiferromagnetic to ferromagnetic transition has also been extracted from these data in a number of ways, and the latter estimates are compared with complementary values deduced from the magnetoresistance data in the following section. Before proceeding with this comparison, some comments on the low-field magnetic response are offered. In the recently reported study[2] of $M(H,T)$ and $\rho(H,T)$ in $Ce(Fe_{0.92}Al_{0.08})_2$, similar features were observed in the low-field magnetization curves acquired at 60 and 80 K (i.e., in the antiferromagnetic phase), which Radha *et al.* suggest might reflect the presence of an impurity phase. While such a possibility remains (despite the fact that this second phase evades detection by other techniques such as x-ray diffraction[2,7]), it might alternatively reflect an intrinsic characteristic of the antiferromagnetic structure, at least near the

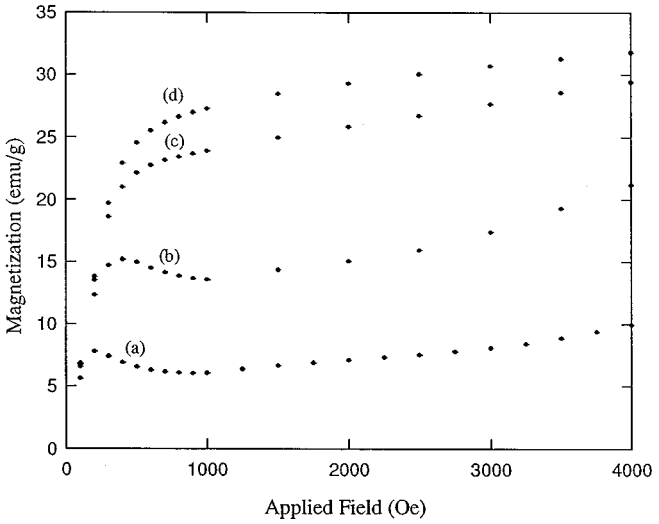

FIG. 4. The lower-field magnetization (in emu/g) plotted against field (in Oe) at fixed temperatures of (a) 109.0 K, (b) 111.0 K, (c) 114.0 K, and (d) 116.8 K.

metamagnetic transition. The feature in question has not only been observed in $Ce(Fe_{0.92}Al_{0.08})_2$ and $Ce(Fe_{0.93}Ru_{0.07})_2$ as mentioned above, but our preliminary measurements on both $Ce(Fe_{0.92}Ru_{0.08})_2$ and Gd_2In (a compound also displaying sequential phase transitions,[13] with comparable magnetic and transport properties) reveal similar features in the low-field response; these characteristics thus appear somewhat ubiquitous. While the low-field slope, $M/H \sim 10^{-3}$ emu/g Oe, of Fig. 3 for $T=67$ K is not inconsistent with the ac susceptibility measured previously,[6,14] it is considerably smaller than the corresponding anomaly in $Ce(Fe_{0.92}Al_{0.08})_2$ (in this latter sample the magnetization in the plateau region is roughly 25% of that measured at 5 T, compared with the 5–10 % ratio evident in Fig. 3); the zero-field susceptibility of this latter system is, however, also enhanced [Mukherjee, Rangahathan, and Roy[5] measured $\chi(0,70\ \mathrm{K})$ at $\sim 10^{-2}$ emu/g Oe in $Ce(Fe_{0.96}Al_{0.04})_2$]. Thus if the measured low-temperature response of these systems is not entirely attributable to some ''impurity'' phase, it must result from some intrinsic, residual orientability of the antiferromagnetic structure in low field. As far as a possible mechanism is concerned, it appears worthwhile recalling that this second transition is induced by doping (resulting in departures from strict stoichiometry), a consequence of which could be that the perturbing potential at the dopant site *might* induce local departures from collinearity amongst the Fe spins. The enhanced magnitude of this effect accompanying Al doping could be a consequence of a stronger local perturbation resulting in the more gradual moment reorientation accompanying the extended overlap between the two phases observed in this system.[1]

More detailed low-field magnetization measurements in the transition region are presented in Fig. 4. Here it is possible to observe the presence of some structure in the low-field response; this structure takes the form of a small but discernible local maximum near 200 and 400 Oe at 109 and 111 K, respectively. At 112.5 K there is just an abrupt change in slope near 500–600 Oe, which gets progressively more rounded with further increases in temperature. Currently we have no quantitative explanation for this structure;

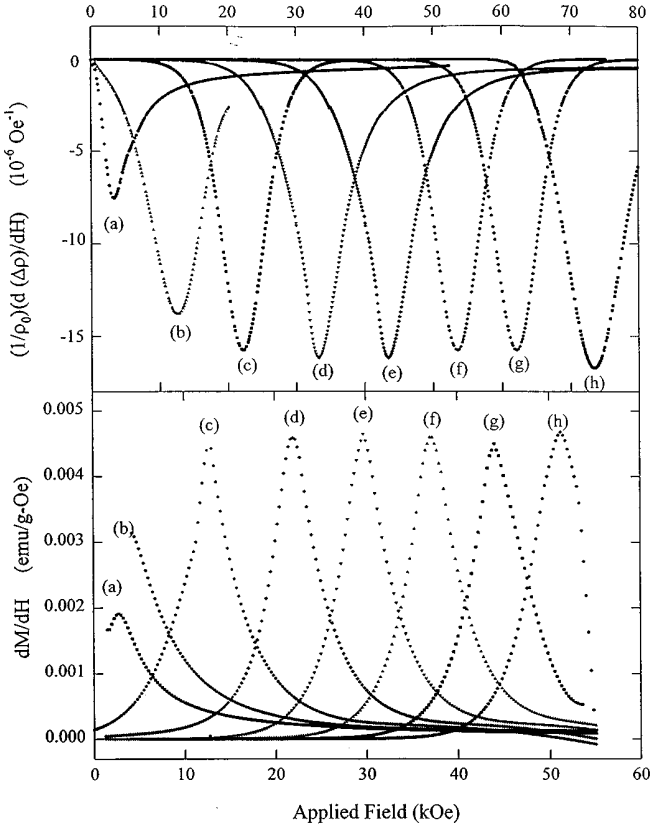

FIG. 5. The derivatives $(1/\rho_0)(d\Delta\rho/dH)$ (in $\mu\mathrm{Oe}^{-1}$) and dM/dH (in emu/g Oe) plotted against the applied field (in kOe) at fixed temperatures of (i), upper figure, (a) 114.1 K, (b) 107.5 K, (c) 101.7 K, (d) 95.3 K, (e) 90.6 K, (f) 84.0 K, (g) 78.2, and (h) 72.6 K, and (ii), lower figure, (a) 114.0 K, (b) 107.5 K, (c) 101.7 K, (d) 95.3 K, (e) 89.7 K, (f) 83.9 K, (g) 78.2 K, and (h) 72.6 K.

we simply note that it appears in a temperature interval close to that at which the coefficient $a_2(T)$ (discussed earlier) for this sample also exhibits an anomaly, although any direct link between the two needs further elucidation. The $Ce(Fe_{0.92}Ru_{0.08})_2$ system is currently being examined for the presence of a similar anomaly.

D. The metamagnetic field $H_m(T)$

The metamagnetic field $H_m(T)$ has been estimated from both the magnetoresistance $\rho(H,T)$ and the magnetization data $M(H,T)$ using two approaches. The first approach, following Radha *et al.*,[2] identifies $H_m(T)$ from the magnetoresistance data as that field at which a negative magnetoresistance first develops, and from the magnetization data as the field (beyond the plateau region discussed in Sec. C above) at which the magnetization begins to increase rapidly. The second method, which is more quantitative in our opinion, is illustrated in Fig. 5; here the derivatives[15] $(\partial M/\partial H)_T$ and $[1/\rho(0,T)](\partial\Delta\rho/\partial H)_T$ [where $\Delta\rho=\rho(0,T)-\rho(H,T)$ represents the field-induced change in resistivity at temperature T] are plotted against the applied field[16] H at a series of fixed temperatures, as closely matched as possible between the two experiments. Here the fields at which the magnitude of these derivatives exhibit maxima are taken as indicating

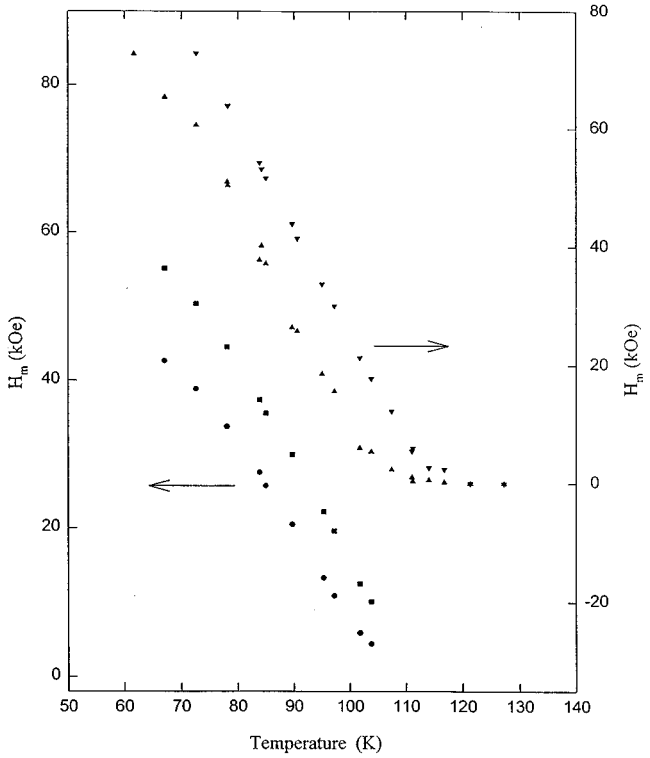

FIG. 6. Estimates of the metamagnetic field $H_m(T)$ (in kOe) plotted against temperature (in K); these estimates were obtained from (i) the onset of a rapid increase in $M(H)$ (●), (ii) the maximum in dM/dH (■), (iii) the onset of a negative $\rho(H)$ (▲), and (iv) the maximum in $d(\Delta\rho)/dH$) (▼).

$H_m(T)$ at that particular temperature. Figure 6 then summarizes the temperature dependence of the four estimates for $H_m(T)$ so obtained.

While these data confirm the general features of the temperature dependence reported[2] for $H_m(T)$ in $Ce(Fe_{0.92}Al_{0.08})_2$, viz., an essentially linear decrease with increasing temperature, specific details are different. By definition, the second method of estimating $H_m(T)$ will invariably yield a larger value than the first approach; nevertheless all *four* estimates for $H_m(T)$ are substantially different at any given temperature and the use of either method on the two sets of measurements [$\rho(H)$ and $M(H)$] yields different values for $H_m(T)$, in contrast to the reported behavior of $Ce(Fe_{0.92}Al_{0.08})_2$. From Fig. 6 it can be seen that three of the four estimates for $H_m(T)$ are well fitted by the form

$$H_m(T) = a(T_N - T), \quad T \leqslant T_N, \tag{1}$$

while the fourth—obtained from the onset of a negative magnetoresistance—displays a little more structure (as indeed do the corresponding estimates in Ref. 2, on close inspection). Here the parameter a varies between about 1.1 and 1.7 kOe/K, dependent on the $H_m(T)$ estimates used, with the derivative-based estimates (a more quantitative measure in our opinion) yielding values in the range 1.3–1.7 kOe/K; the latter are significantly larger[18] than the 0.9 kOe/K found in the Al-doped system,[2] but reasonably close to the value of 1.6 kOe/K suggested by related experiments[17] on $Ce(Fe_{0.8}Co_{0.2})_2$. It is also interesting to note that the T_N

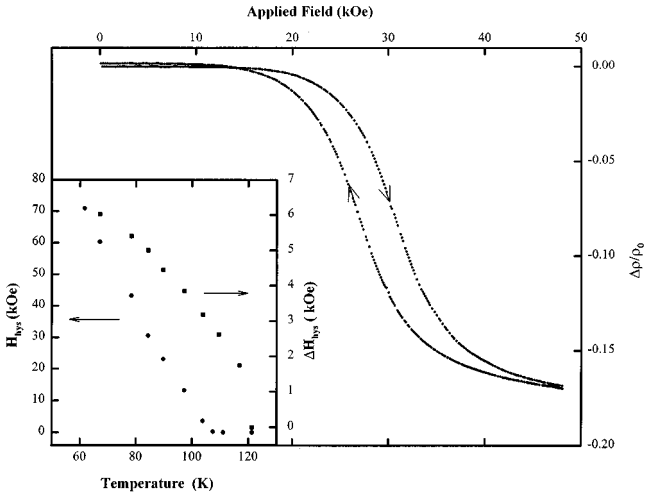

FIG. 7. The fractional magnetoresistance $\Delta\rho/\rho_0$ plotted against applied field (in kOe), showing hysteresis effects, at a fixed temperature of 78.2 K. The inset shows the field beyond which hysteresis occurs, $H_{\rm hys}$ (in kOe), and the width $\Delta H_{\rm hys}$ of the hysteresis loop (both determined from resistivity data), plotted against temperature (in K).

estimates found by fitting the data in Fig. 6 to Eq. (1) fall in the range 107–115 K, with the estimates employing the second (derivative) $H_m(T)$ values yielding $T_N \sim 112$–115 K; the latter, in particular, are in excellent agreement with both the temperature interval (112–117 K) over which the coefficient $a_2(T)$ (for the sample) exhibits[6] a peak and the onset temperature for the zero-field resistive transition ($\sim$116 K).

E. Hysteretic behavior

A summary of the hysteretic behavior displayed by the $Ce(Fe_{0.93}Ru_{0.07})_2$ system is presented in Fig. 7; the study of hysteresis in this system has concentrated primarily on the magnetoresistive behavior, due to the wider field range available in that experiment. From data similar to those illustrated in this last figure, two parameters have been extracted: (i) the field $H_{\rm hys}(T)$ beyond which hysteresis first appears at a given temperature [or, alternatively, the field below which the hysteresis in $\rho(H)$ disappears], and (ii) the maximum width in field $\Delta H_{\rm hys}(T)$ of the hysteresis ''loop,'' i.e., the $\rho(H)$ vs H plot. The temperature dependence of these two fields is summarized in the inset in Fig. 7. From this figure it can be seen that while the field $H_{\rm hys}(T)$ for the onset of hysteresis becomes nonzero near 108 K [so that it is tempting to suggest that hysteretic behavior occurs at or just below the onset of the metamagnetic transition, as in[2] $Ce(Fe_{0.92}Al_{0.08})_2$], the width $\Delta H_{\rm hys}(T)$ of the loop—a direct measure of the actual presence of hysteresis—approaches zero near 121 K, slightly above both the onset of the zero-field resistive transition ($\sim$116 K) and the extrapolated location for T_N [$\leqslant$115 K, Fig. 6, although the largest $H_m(T)$ estimates vanish only above 117 K].

As a final comment on this hysteretic behavior it should be noted that the flattening evident in the width $\Delta H_{\rm hys}(T)$ at lower measuring temperatures probably reflects the inability of the highest available applied field to achieve saturation there.

IV. SUMMARY AND CONCLUSIONS

A detailed study of the temperature- and field-dependent resistivity and magnetization of $Ce(Fe_{0.93}Ru_{0.07})_2$ has been carried out in the vicinity of the ferromagnetic to antiferromagnetic transition. Applied fields basically displace T_N and the associated jump in the resistivity to lower temperatures, and it is the field-induced metamagnetic transition that is the cause of GMR in this system. Nevertheless, while the *mechanism* underlying GMR is well established in this system (a mechanism that appears to be shared with a variety of other intermetallic compounds[19] in which, furthermore, it might be thought an understanding of GMR would be easier to achieve than in multilayer systems where complications can arise from interfacial scattering), a quantitative *model* description for this behavior is still lacking, as the following indicates. Itinerant models[20] appear capable of reproducing the essentially linear boundary in the (H-T) plane between the ferromagnetic and antiferromagnetic phases evident in this (Fig. 6) and related systems;[2,17] however, a quantitative link between resistivity and magnetization is difficult to establish within such an approach. An attempt has therefore been made to correlate the behavior of $\rho(H,T)$ and $M(H,T)$ in terms of localized model predictions, viz., the so-called ''s-d'' model[21] in which such a correlation appears implicitly. This model leads to a field-induced change in resistivity $\Delta\rho(H,T)=\rho(0,T)-\rho(H,T)$ of the form[22]

$$\Delta\rho(H,T)=Ac\left[J^2\langle S_z\rangle\tanh\left(\frac{\alpha}{2}\right)+\frac{4V^2J^2\langle S_z\rangle^2}{V^2+J^2[S(S+1)-\langle S_z\rangle\tanh(\alpha/2)]}\right], \quad (2)$$

where $A(=3\pi m^*\Omega/2\hbar e^2E_F)$ incorporates details of the band structure (m^* being the conduction-electron effective mass, E_F the corresponding Fermi energy, and Ω the atomic volume). Of the remaining parameters, c indicates the atomic fraction of scattering sites, and the parameter α is dimensionless ($\alpha=g\mu_BH_i/k_BT$ where H_i represents the internal field which, in principle, could be site dependent). $\langle S_z\rangle$ has simply been taken as the measured magnetization (thus containing contributions from Fe and Ce moments), while the parameters $|V|$ and $|J|$ (representing, respectively, the spin-independent potential at scattering sites and the exchange coupling constant between conduction-electron and localized spins) have been allowed to vary freely in an attempt to minimize the deviation between model curves and the data.[23] The fits associated with this approach are summarized in Fig. 8, in which the internal field H_i has been set, respectively, at (a) the applied field H_a and (b) the sum of H_a and a constant ''molecular'' field H_m ($=k_BT_N/\mu_B$), while (c) utilizes a variable effective field $H_i=H_a+\lambda M$, with $\lambda=T_N$. Such an approach has obvious shortcomings; nevertheless, it highlights the difficulties associated with attempts to provide a quantitative representation of these data using localized models. As is clear from Fig. 8, none of the approximations adopted produces an acceptable fit to these data; while all of the model curves yield a strong negative magnetoresistance, the onset of this effect occurs at markedly *lower* applied fields than is observed experimentally. This disagreement originates directly from the use of the measured magnetization in Eq. (2); this shows a rapid increase at a field which is always lower than that at which the magnetoresistance displays a sharp decrease. While more sophisticated models exist[19] in which both the magnetic scattering component [approximated by Eq. (2) here] and the nonmagnetic contribution to the resistivity are combined with factors of the form $[1-gm(T)]$ [where $m(T)$ is the staggered sublattice magnetization characterizing the antiferromagnetic phase and g reflects the reduction in the effective number of conduction electrons due to gaps in the electronic energy spectrum near E_F resulting from superzone effects], the applicability of such models cannot be assessed quantitatively at present as no estimates for $m(T)$ are available. However, on qualitative grounds, they are unlikely to improve model fits as it is difficult to understand why significant changes in the measured magnetization $M(T)$ would occur at field strengths which are different from those at which corresponding changes in the sublattice magnetization $m(T)$ are occurring.

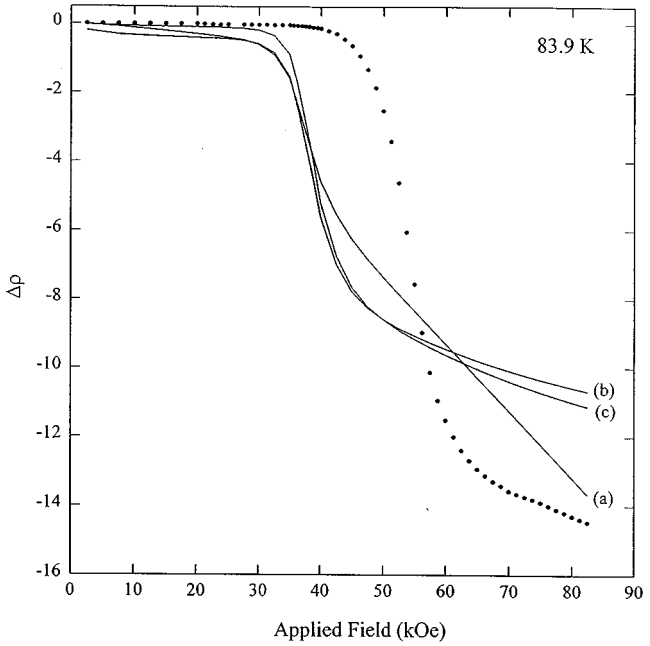

FIG. 8. The magnetoresistance $\Delta\rho=\rho(H,T)-\rho(0,T)$ (in $\mu\Omega$ cm) plotted against applied field (in kOe) at 83.9 K. (●) represents the experimental data while the three curves labeled (a), (b), and (c) utilize the corresponding approximations for the internal field H_i discussed in the text. Additionally, in curve (a) $|J|=1.29$ eV and $|V|=0.16$ eV, in curve (b) $|J|=0.24$ eV and $|V|=0.25$ eV, and in curve (c) $|J|=0.27$ eV and $|V|=0.17$ eV.

ACKNOWLEDGMENTS

Support for this work from various programs of the Natural Sciences and Engineering Research Council (NSERC) of Canada is gratefully acknowledged. The work at MSU was supported by the NSF and the MSU Center for Fundamental Materials Research. One of us (G.W.) would like to thank the Condensed Matter Physics group at Michigan State University for support and hospitality during a leave in which the magnetization data were collected.

[1] A. K. Rastogi and A. P. Murani, in *Theoretical and Experimental Aspects of Valence Fluctuations and Heavy Fermions*, edited by L. C. Gupta and S. K. Malik (Plenum, New York, 1987); S. J. Kennedy, A. P. Murani, B. R. Coles, and O. Moze, J. Phys. F **18**, 2499 (1988); S. J. Kennedy, A. P. Murani, J. K. Cockcroft, S. B. Roy, and B. R. Coles, J. Phys. Condens. Matter **1**, 629 (1989); S. J. Kennedy and B. R. Coles, *ibid.* **2**, 1213 (1990); S. J. Kennedy, P. J. Brown, and B. R. Coles, *ibid.* **5**, 5169 (1993).

[2] S. Radha, S. B. Roy, A. K. Nigam, and G. Chandra, Phys. Rev. B **50**, 6866 (1994).

[3] A. K. Nigam, S. Radha, S. B. Roy, and G. Chandra, Physica B **205**, 421 (1995).

[4] S. B. Roy and B. R. Coles, J. Phys. Condens. Matter **1**, 419 (1989).

[5] S. Mukherjee, R. Ranganathan, and S. B. Roy, Phys. Rev. B **50**, 1084 (1994).

[6] D. Wang, H. P. Kunkel, and G. Williams, Phys. Rev. B **51**, 2872 (1995).

[7] S. B. Roy and B. R. Coles, Phys. Rev. B **39**, 9360 (1989).

[8] W. B. Muir and J. O. Ström-Olsen, J. Phys. E **9**, 163 (1976).

[9] C. J. Schinkel, R. Hartog, and F. H. A. M. Hochstenbach, J. Phys. F **4**, 1412 (1974); P. A. Algarabel, M. R. Ibarra, C. Marquina, A. del Moral, J. Galibert, M. Iqbal, and S. Askenzay, Appl. Phys. Lett. **66**, 3062 (1995).

[10] J. W. F. Dorleijn, Philips Res. Rep. **31**, 289 (1976).

[11] H. Rakoto, H. C. Ousset, S. Senoussi, and I. A. Campbell, J. Magn. Magn. Mater. **46**, 212 (1984).

[12] K. H. J. Buschow, in *Ferromagnetic Materials*, edited by E. P. Wohlfarth (North-Holland, Amsterdam, 1980), Vol. 1, p. 297 *et seq*.

[13] S. P. McAlister, J. Phys. F **14**, 2167 (1984); M. Saran, G. Williams, and S. P. McAlister, Solid State Commun. **57**, 53 (1986).

[14] D. Wang, M.Sc. thesis, University of Manitoba, 1994.

[15] These derivatives were calculated by fitting the experimental $\rho(H,T)$ and $M(H,T)$ versus H curves with a ''best fit'' analytic expression (chosen from amongst some 3000 arbitrary functions in a TABLECURVE routine—these functions have no physical relevance) and then differentiating the expression adopted.

[16] Since the same specimen, mounted in the same orientation, was used in both experiments, there is a one-to-one correspondence between the applied and internal fields in *both* sets of data.

[17] N. Ali and X. Zhange, J. Phys. Condens. Matter **4**, L351 (1992); these authors measured the field dependence of T_N, and find $T_N(H)-T_N(0)\sim a'H$ with $a'=-0.64$ K/kOe; a' corresponds to a^{-1} in Eq. (1).

[18] A more appropriate comparison would be, of course, between the corresponding internal fields. However, for the sample shape adopted in the present experiment such a correction is small, amounting to 2% or less.

[19] V. Sechovsky, L. Havela, K. Prokes, H. Nakotte, F. R. de Boer, and E. Brück, J. Appl. Phys. **76**, 6913 (1994).

[20] T. Moriya and K. Usami, Solid State Commun. **23**, 935 (1977); T. Moriya, *Spin Fluctuations in Itinerant Electron Magnetism* (Springer, Berlin, 1985).

[21] K. Yosida, Phys. Rev. **107**, 396 (1957).

[22] J. Bews, A. W. Sheikh, and Gwyn Williams, J. Phys. F **16**, 1537 (1986).

[23] The prefactor Ac has been set, somewhat arbitrarily, at 200 $\mu\Omega$ cm, a value which could result typically from taking c as 0.67, the fraction of effective (Fe) scattering sites, and A as about 3 $\mu\Omega$ cm/at. % Fe; this choice is not critical as changes in it will simply be complemented by changes in $|V|$ and $|J|$.